Pergamon PII: S0038–092X(00)00085–2

Solar Energy Vol. 69, No. 4, pp. 343–350, 2000

Printed in Great Britain
0038-092X/00/$ - see front matter

www.elsevier.com/locate/solener

ANN BASED PEAK POWER TRACKING FOR PV SUPPLIED DC MOTORS

MUMMADI VEERACHARY*,†,‡ and NARRI YADAIAH**
*Dept. of Electrical Engineering, Jawaharlal Nehru Technological University, College of Engineering, Anantapur, 515 002, Andhra Pradesh, India
**School of Continuing & Distance Education, Jawaharlal Nehru Technological University, Masab Tank, Hyderabad, 500 028, Andhra Pradesh, India

Received 6 September 1999; revised version accepted 6 April 2000

Communicated by HANSJÖRG GABLER

Abstract—This paper presents an application of an Artificial Neural Network (ANN) for the identification of the optimal operating point of a PV supplied separately excited dc motor driving two different load torques. A gradient descent algorithm is used to train the ANN controller for the identification of the maximum power point of the Solar Cell Array (SCA) and gross mechanical energy operation of the combined system. The algorithm is developed based on matching of the SCA to the motor load through a buck-boost power converter so that the combined system can operate at the optimum point. The input parameter to the neural network is solar insolation and the output parameter is the converter chopping ratio corresponding to the maximum power output of the SCA or gross mechanical energy output of the combined PV system. The converter chopping ratios at different solar insolations are obtained from the ANN controller for two different load torques and are compared with computed values. © 2000 Published by Elsevier Science Ltd.

1. INTRODUCTION

The rapid trend of industrialization of nations, increased interest in environmental issues led recently to explore the use of renewable forms such as solar energy. Photovoltaic (PV) generation is gaining increased importance as renewable source due to its advantages like absence of fuel cost, no noise and wear due to absence of moving parts and little maintenance etc. In particular PV systems are rapidly expanding and have increasing roles in electric power technologies, providing more secure power sources to the pumping systems, where it is not economically viable to connect the existing grid supply. Optimum operation (Zinger and Braunstein, 1981) of the SCA and a dc shunt motor is achieved by means of a switching procedure of the SCA modules, direct current transformers as well as controlling the motor fluxes. Appelbaum (1986) has analyzed the performance of dc motors (separately, series and shunt) supplied from PV sources. These studies reveal that the dc shunt motor powered by solar cells has an inferior performance and a separately excited dc motor driving a centrifugal pump is the best device/drive as far as better matching of the PV generator is concerned. Performance analysis (dynamic and steady state) of dc motors fed from PV supplies through intermediate power converter have been reported (Veerachary, 2000). Saied (1988) formulated guidelines to construct the motor v-i characteristics for maximum daily gross mechanical energy output (GME) and to determine the optimal motor parameters to match the solar generator.

Artificial Neural Networks are widely accepted as a technology offering an alternative way to solve complex problems and have been successfully applied in many areas. The power of the ANNs in modeling complex mappings and in system identification has been demonstrated (Narendra and Parthasarathy, 1990). ANN based real time maximum power tracking controller for PV grid connected systems has been reported (Takashi and Imakubo, 1995). The studies emphasize that the SCA operating point is shifted to its maximum power point by using a voltage control type inverter, which is identified by the ANN. Various methods of maximum power (MP) tracking have been reported in literature. Of these, the perturbation and observation method, which is popular for slowly varying solar insolations, moves the operating point towards the maximum power point by periodically increasing or decreas-

†Author to whom correspondence should be addressed; e-mail: charymv@mailcity.com
‡Presently at Dept. of Electrical and Electronics Engg, University of Ryakyus, 1 Senbaru, Nishihara, Nakagami, Okinawa 903-0213, Japan.

ing the array voltage. On the other hand the incremental conductance method offers good performance under rapidly changing solar insolations, but it requires the high-resolution sensors for measurement and the aspect of instrumentation imposes an economic constraint.

The present paper brings out the identification of optimal point (corresponding to MP or GME operation) of the PV supplied separately excited dc motor fed from intermediate power converter driving centrifugal pump or volumetric pump loads. The converter-chopping ratio is selected adaptively using ANN to get maximum power from SCA or GME output from the combined system. This on-line training approach avoids adjustment of optimal operating point through trial and error procedure and does not require high-resolution sensors.

The paper is organized as follows: In Section 2 problem statement is given. Section 3 deals with development of mathematical models for individual blocks like, PV generator, dc motor, power converter and pump loads. In Section 4 ANN structure and its algorithm for designing an adaptive controller is presented. Results and conclusions follow in the final section of this paper.

2. STATEMENT OF PROBLEM

The problem is to design an adaptive controller by using Artificial Neural Network for obtaining the MP or GME operation of the PV supplied dc motor system. These MP or GME operations can be achieved at different solar insolations by controlling the power converter duty ratio, which is adjusted by the adaptive ANN controller.

3. MATHEMATICAL MODEL OF THE SYSTEM

The combined system mainly consists of Solar Cell Array, dc–dc converter, dc motor coupled to either centrifugal pump or volumetric pump load as shown in Fig. 1. Mathematical model for individual components and describing equations for MP, GME operations are derived in the following sections.

3.1. PV generator model

The PV generator is formed by the combination of many PV cells connected in series and parallel fashion to provide desired value of output voltage and current. This PV generator exhibits a nonlinear insolation dependent v-i characteristic. The

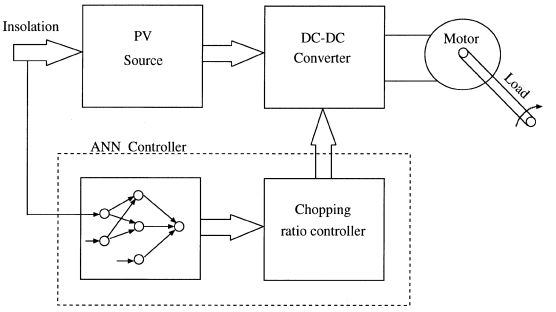

Fig. 1. Functional block diagram of the system.

v-i characteristic (Appelbaum, 1986) with N_s cells in series and N_p cells in parallel is

$$V_g = -I_g R_s\left(\frac{N_s}{N_p}\right) + \left(\frac{N_s}{\Lambda}\right)\ln\left\{1 + \left(\frac{N_s I_{ph} - I_g}{N_p I_o}\right)\right\} \tag{1}$$

where $\Lambda = q/AKT$; q–electric charge; A–Completion factor; K–Boltzman constant; T–Absolute temperature. The equivalent circuit of PV generator is shown in Fig. 2. Fig. 3 shows the output v-i, P-i characteristics of the solar cell array (insolation of 1000 W/m^2 = 100% insolation) with solar insolation as a parameter. In this figure I_g, V_g, and P_g are the output current, voltage and power of the solar array respectively. It is seen that in Fig. 3 the maximum power point of the solar array shifts when the solar insolation is changing. The PV generator considered in these studies consists of 18 parallel paths and each path contains 324 cells in series. After substituting the cell constants in Eq. (1) and upon simplification the resulting v-i characteristic is

$$V_g = -0.9 I_g + 23.697 \ln\{1.0 + 123.456(13.45\, K_{ins} - I_g)\} \tag{2}$$

where K_{ins} is percentage of insolation.

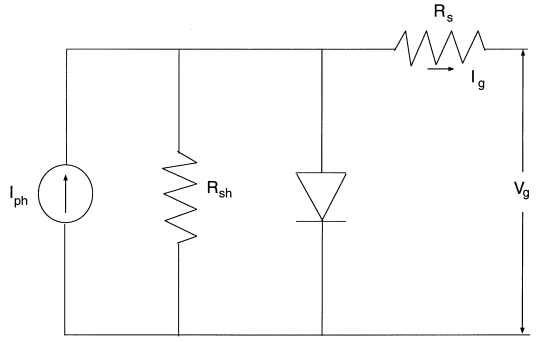

Fig. 2. Equivalent circuit of the PV generator.

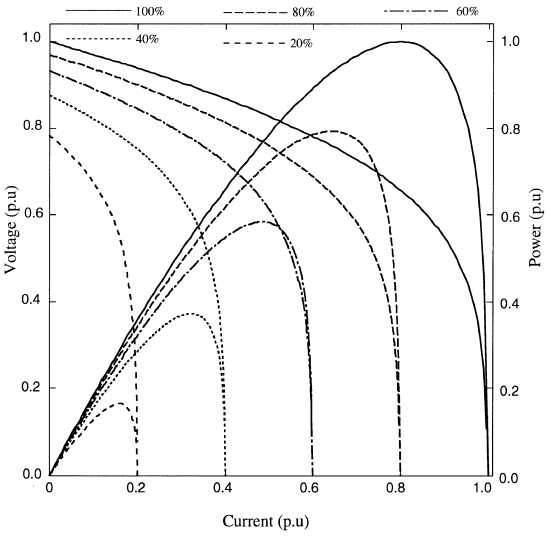

Fig. 3. The v-i/P-i characteristics of PV generator at different solar insolations.

3.2. Power converter model

The intermediate dc–dc converter is a buck-boost converter with a variable duty or chopping ratio. This converter produces a chopped output dc voltage and controls the motor average voltage, current. Further, the converter continuously matches the output characteristic of the PV generator to the input characteristic of the motor so that maximum power is extracted from the SCA or the gross mechanical energy per day of the system is maximum. Assuming the dc–dc converter is ideal, the output voltage and current of the converter for a duty ratio 'δ' is related to the solar cell voltage (V_g), current (I_g) as

$$V_{av} = \frac{\delta V_g}{(1-\delta)} \tag{3}$$

$$I_{av} = \frac{I_g(1-\delta)}{\delta} \tag{4}$$

$$\delta = \left(\frac{t_{on}}{T_p}\right) \tag{5}$$

$$Y = \frac{\delta}{(1-\delta)} \tag{6}$$

where δ–duty ratio; Y–chopping ratio; T_p–switching period of the converter; $\delta < 0.5$ for buck operation and $\delta > 0.5$ for boost operation.

3.3. Model of the dc motor

When the dc separately excited motor is supplied from a PV source through an intermediate power modulator, the motor voltage and torque equations under steady-state are

$$V_{av} = E_b + I_{av}R_a \tag{7}$$

$$T_e = C_e I_{av} \tag{8}$$

$$E_b = C_e \omega \tag{9}$$

3.4. Model for the pump-loads

Pumps may be volumetric or centrifugal types having different head–vs.–flow characteristics. These pump loads will develop speed dependent torques. The speed–torque characteristics of centrifugal (T_{L1}) and volumetric pump (T_{L2}) loads including friction torque are given by

$$T_{L1} = A_1 + B_1\omega + C_1\omega^{1.8} \quad \text{Nm} \tag{10A}$$

$$T_{L2} = A_1 + B_1\omega \quad \text{Nm} \tag{10B}$$

3.5. Maximum power operation of SCA

For maximum utilization of SCA, a power converter is introduced in between SCA and motor. The duty ratio of the converter is changed accordingly to match the motor load to SCA. Assuming the power converter is ideal (all of the array power is delivered to the motor) at maximum power point, the power absorbed by the motor is equal to the power delivered by the SCA i.e.

$$P_m = V_{av}I_{av} = V_m I_m \tag{11}$$

where V_{av}, I_{av} are the motor armature voltage, current; V_m, I_m are SCA voltage, current respectively at maximum power point of SCA. The motor armature voltage and currents are expressed in terms of SCA voltage, current at maximum power point as

$$V_{av} = \delta_{mp}V_m \tag{12}$$

$$I_{av} = \frac{I_m}{\delta_{mp}} \tag{13}$$

$$V_{av} = E_b + I_{av}R_a \tag{14}$$

From Fig. 4 transforming the motor equivalent circuit to SCA side by substituting Eq. (12) and

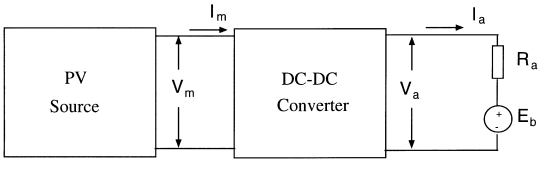

Fig. 4. Equivalent circuit of the combined system.

Eq. (13) in Eq. (14) then the motor armature voltage equation (in terms of SCA voltage, current) is

$$V_m = \frac{E_b}{\delta_{mp}} + I_m \frac{R_a}{\delta_{mp}^2} \tag{15}$$

Rearranging the above equation

$$V_m \delta_{mp}^2 - E_b \delta_{mp} - I_m R_a = 0 \tag{16}$$

for the above equation two solutions exist. Since the duty ratio never be negative, expression which gives positive duty ratio is

$$\delta_{mp} = \frac{E_b}{2V_m} + \left(\left(\frac{E_b}{2V_m} \right)^2 + \left(\frac{I_m R_a}{V_m} \right) \right)^{1/2} \tag{17}$$

For a given SCA maximum power, the motor armature current is obtained from the following equations

$$P_m = E_b I_{av} + I_{av}^2 R_a \tag{18}$$

$$R_a I_{av}^2 + E_b I_{av} - P_m = 0$$

$$I_{av} = -\frac{E_b}{2V_m} + \left(\left(\frac{E_b}{2V_m} \right)^2 + \left(\frac{P_m}{R_a} \right) \right)^{1/2} \tag{19}$$

where E_b is given by Eq. (9). The duty ratio of the converter (Eq. (17)) depends on the motor back emf, which in turn depends on the motor load. When the dc motor coupled to the load (centrifugal or volumetric pump-load) the back emf at a given SCA power (P_m) is obtained by solving ($T_e = T_L$) Eqs. (8), (10-A), and Eqn. (19) in case of centrifugal pump load and Eqn. (8), Eqn. (10-B), and Eqn. (19) for volumetric pump load. Once back emf is calculated corresponding to P_m, the duty ratio of the converter is obtained from Eqn. (17). These computed values are taken as reference patterns for training the Neural Network.

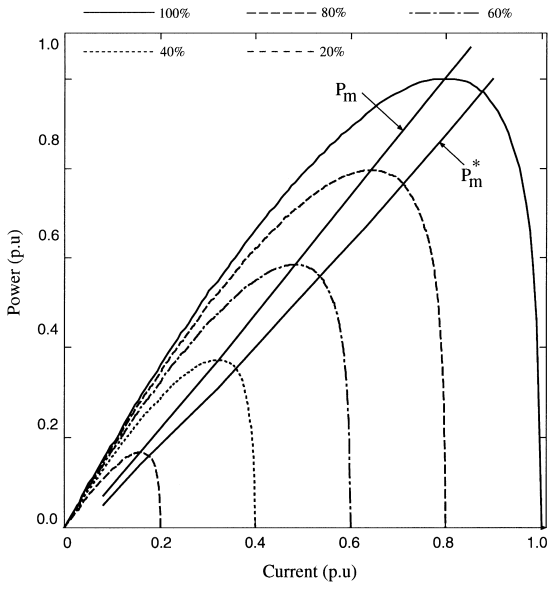

Fig. 5. MP and GME operating points trajectory of SCA at different solar insolations.

3.6. Maximum gross mechanical energy output from SCA

For a given value of flux coefficient of the machine it is not possible to make the SCA and motor to operate at maximum power points (P_m, V_m, I_m) at all solar insolations. This is because of the motor v-i characteristic dependent on motor flux coefficient and copper losses in the machines. In such cases the system is made to operate at a point (P_m^*, V_m^*, I_m^*) of gross mechanical energy output per day for a given daily insolation curve. The operating point's trajectory is shown in Fig. 5. At these operating points $V_m^* > V_m$, $I_m^* < I_m$. For the machine under consideration the optimal parameters $C_e = 0.6626$ (Saied, 1988) make the combined system operate at maximum gross mechanical energy output. At a given solar insolation the voltage and current (V_m, I_m) corresponding to MP operation are determined. With these V_m, I_m the voltage and currents (V_m^*, I_m^*) corresponding to GME operation are computed using the following equations.

$$V_m^* = \frac{V_m (2R_a + 89.8 I_m^{0.127})}{(R_a + I_m^{0.127})} \tag{20}$$

$$I_m^* = \frac{89.8 I_m^{0.873}}{(R_a + I_m^{0.127})} \tag{21}$$

$$P_m^* = V_m^* I_m^* \tag{22}$$

$$I_{av}^* = -\frac{E_b^*}{2V_m} + \left(\left(\frac{E_b^*}{2V_m} \right)^2 + \left(\frac{P_m^*}{R_a} \right) \right)^{1/2} \tag{23}$$

where back emf (E_b^*) is calculated using Eqn. (8), Eqn. (10-A), and Eqn. (23) in case of centrifugal pump load; Eqn. (8), Eqn. (10-B), and Eqn. (23) in case of volumetric pump load at different solar insolations. Knowing E_b^* the duty ratio of the buck-boost converter for GME operation is obtained from the following equation.

$$\delta^*_{mg} = \frac{E^*_b}{2V^*_m} + \left(\left(\frac{E^*_b}{2V^*_m} \right)^2 + \left(\frac{I^*_m R_a}{V^*_m} \right) \right)^{1/2} \quad (24)$$

4. ARTIFICIAL NEURAL NETWORKS

Artificial neural networks are widely accepted as a technology offering an alternative way to solve complex and ill-defined problems. ANNs are the gross simplification of real biological networks and mimic somewhat the learning process of a human brain. According to Haykin (1994), an ANN is a massively parallel distributed processor that has a natural propensity for storing experimental knowledge and making it available for use. It resembles the human brain in two respects, the network through a learning process acquires the knowledge, and the synaptic weights are used to store the knowledge. The typical ANN models are composed of many non-linear computational elements operating in parallel and arranged in different structures to resemble the biological neural networks as shown in Fig. 6. The capacity of a neural network is of little utility unless it is accompanied by useful generalizations to patterns that are not presented during training. In fact, if generalization is not needed, we can simply store the associations in a look-up table, and thus neural networks may be of little importance (Widrow and Lehr, 1990).

ANN models represent a new method in system identification and provide attractive alternatives for development of adaptive controllers. These ANNs operate like a black box model, requiring no detailed information about the system. Instead, they learn the relationship between the input parameters, controlled and uncontrolled variables by studying previously recorded data, and similar to the way a non-linear regression might perform. Another advantage of using ANN's is their ability to handle large and complex systems with many interrelated parameters. They seem to simply ignore excess input data that are of minimal significance and concentrate instead on the more important inputs. This trained ANN can be used to approximate an arbitrary input–output mapping of the system.

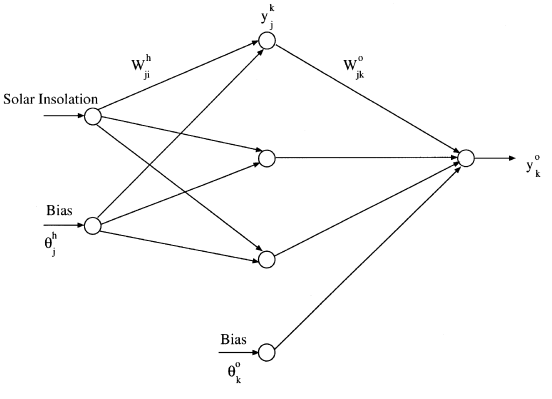

Fig. 6. Schematic diagram of a artificial neural network.

We now begin by considering the feed forward neural network consisting of single hidden layer. The selection of activation function plays an important role in designing neural network. In the present problem a bipolar sigmoid function f[u(t)] = tanh[g.u(t)] for the hidden layer, linear function f[u(t)] = g.u for the output layer were considered and the network is expressed by the following set of equations:

An input vector, $x = (x_1, x_2, x_3, \ldots, x_n)^t$ is applied to the input layer of the network. The net input to the hidden 'j' unit is:

$$net^h_j = \sum_{i=1}^{n} w_{ji} x_i + \theta^h_j \quad (25)$$

where W^h_{ji} is the weight on the connection from i^{th} input unit, θ^h_j for $j = 1, 2, \ldots, N_h$ represents the bias for hidden layer neurons. Now, the output of the neurons in the hidden layer may be written as

$$y^h_j = f\left(\sum_{i=1}^{n} w_{ji} x_i + \theta^h_j \right) \quad (26)$$

and the net input to the neurons in the output layer becomes

$$net^o_k = \sum_{j=1}^{N_h} w_{kj} y^h_j + \theta^o_k \quad (27)$$

where θ^o_k represents the bias for neurons in the output layer. Finally the output of the neurons in the output layer is

$$y^o_k = f\left(\sum_{j=1}^{N_h} w_{kj} y^h_j + \theta^o_k \right) \quad (28)$$

With the above equations in the forward direction, the error propagation rule (Rumelhart et al., 1986; Freeman and Skapura, 1991) is used in the following steps:

Step 1. Construct the network and initialize the synaptic weights with random values.

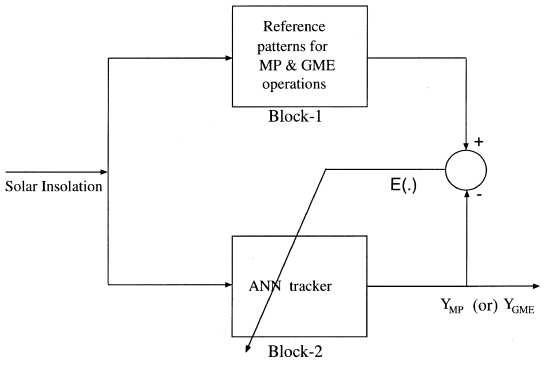

Fig. 7. Block diagram for ANN training.

Step 2. Apply an input vector to the network and calculate the corresponding output values (eqn(25) to Eqn. (28)).

Step 3. Compare the actual outputs with the desired outputs and determine a measure of the error.

Step 4. Determine the amount by which each weight is to be changed and make corrections to each weight.

Step 5. Repeat step 2 to step 4 with all the training vectors until the error for the vectors in the training set is reduced to an acceptable value.

The ANN training block diagram for MP or GME operation is shown in Fig. 7. Using the mathematical models developed in Sections 3.5 and 3.6 the reference patterns for MP and GME operation are computed. Block-1 represents these reference patterns. The ANN training is performed by initially assigning random values to the weight terms. Gradient descent algorithm is used in the training, as it improve the performance of the ANN by reducing the total error by changing the weights along its gradient. The learning rate is 0.55 and momentum factor 0.80 is selected for satisfactory training. The training process was terminated as and when the mean square error $E(.)$ is less than the specified value.

Table 1. Machine data

V	120 Volts
I	9.2 A
Speed	1500 rpm
R_a	1.50 Ω
L_a	0.02 H
C_e	0.6626
J	0.0236
A_1	0.00039
B_1	0.00238
C_1	0.50000

5. RESULTS AND CONCLUSIONS

A 120V, 9.2A, 1500 rpm PV supplied dc separately excited motor driving (i) centrifugal pump load (ii) volumetric pump load is considered in these studies. The parameters of the machine, PV generators are given in Table 1 and 2 respectively. Based on the mathematical models developed in the preceding Sections (3.5 and 3.6) the converter chopping ratios are computed for (i) maximum power operation of SCA (ii) gross mechanical energy output operation at different solar insolations for two load torques mentioned above. The computed values for the above two cases are tabulated in Table 3. Following the procedure outlined in Section 4 the ANN is trained starting with random synaptic weights. The training data for the network is taken from Table 3. The chopping ratios corresponding to MP & GME operations are obtained from this trained adaptive ANN controller for different solar insolations (from 10–100% solar insolation in steps of 5%). The results of MP & GME operations are given for comparison purpose in Tables 4 and 5 respectively. It can be seen from these results that the computed and predicted values of chopping ratios are closely matching. Further the percentage error in the computation of chopping ratio from ANN controller is tabulated in Tables 6 and 7. From these results it can be seen that the error in ANN prediction is less than 2%, 7% for centrifugal, volumetric pump loads respectively. It is observed from the studies that the ANN even though trained for ten solar insolations the intermediate results obtained from the network are within the range.

The adaptive controller using ANN is tested for different set of solar insolations and the results are close to the computed values. The developed controller can also be extended for PV supplied PM and series motors. From these studies it is found that the ANN provides a highly accurate identification/tracking of optimal operating points even with stochastically varying solar insolations.

Table 2. PV generator data

Λ_g	0.0422 Volt^{-1}
I_{og}	0.0081 A
J	0.0236
N_s	326
N_p	18

Table 3. Computed values of chopping ratios

% Of solar insolation	Chopping ratio with maximum power operation (Y_{MP})		Chopping ratio with gross mechanical operation (Y_{GME})	
	Volumetric pump load	Centrifugal pump load	Volumetric pump load	Centrifugal pump load
10	0.1634	0.5196	0.1741	0.5530
20	0.3201	0.6526	0.3413	0.6814
30	0.4711	0.7410	0.5028	0.7866
40	0.6167	0.8105	0.6589	0.8582
50	0.7708	0.8846	0.8247	0.9359
60	0.9061	0.9342	0.9710	0.9876
70	1.0501	0.9919	1.1271	1.0476
80	1.1766	1.0324	1.2648	1.0889
90	1.2991	1.0704	1.3990	1.1287
100	1.4305	1.1186	1.5434	1.1784

Table 4. Comparison of chopping ratios (Y_{MP}) for MP operation

% of Solar insolation	Volumetric pump load		Centrifugal pump load	
	Computed chopping ratio	Predicted from ANN controller	Computed chopping ratio	Predicted from ANN controller
10	0.1634	0.1743	0.5196	0.5256
15	0.2351	0.2488	0.5769	0.5779
20	0.3201	0.3234	0.6526	0.6390
25	0.3891	0.3978	0.6876	0.6976
30	0.4711	0.4720	0.7410	0.7448
35	0.5515	0.5458	0.7875	0.7831
40	0.6167	0.6192	0.8105	0.8176
45	0.7070	0.6920	0.8491	0.8504
50	0.7708	0.7642	0.8846	0.8803
55	0.8458	0.8355	0.9175	0.9070
60	0.9061	0.9062	0.9342	0.9333
65	0.9787	0.9758	0.9638	0.9609
70	1.0501	1.0444	0.9919	0.9884
75	1.1073	1.1119	1.0065	1.0134
80	1.1766	1.1783	1.0324	1.0368
85	1.2446	1.2434	1.0572	1.0599
90	1.2991	1.3072	1.0704	1.0805
95	1.3654	1.3697	1.0937	1.0956
100	1.4305	1.4308	1.1186	1.1046

Table 5. Comparison of chopping ratios (Y_{GME}) for GME operation

% of Solar insolation	Volumetric pump load		Centrifugal pump load	
	Computed chopping ratio	Predicted from ANN controller	Computed chopping ratio	Predicted from ANN controller
10	0.1741	0.1833	0.5515	0.5530
15	0.2506	0.2638	0.6122	0.6133
20	0.3413	0.3443	0.6922	0.6814
25	0.4151	0.4247	0.7291	0.7412
30	0.5028	0.5049	0.7853	0.7866
35	0.5891	0.5847	0.8341	0.8237
40	0.6589	0.6641	0.8582	0.8614
45	0.7425	0.7428	0.8987	0.9018
50	0.8247	0.8209	0.9359	0.9391
55	0.9057	0.8982	0.9704	0.9680
60	0.9710	0.9745	0.9876	0.9900
65	1.0496	1.0497	1.0185	1.0112
70	1.1271	1.1238	1.0476	1.0369
75	1.1894	1.1968	1.0627	1.0681
80	1.2648	1.2684	1.0889	1.0998
85	1.3393	1.3387	1.1152	1.1250
90	1.3990	1.4075	1.1287	1.1413
95	1.4717	1.4748	1.1527	1.1505
100	1.5434	1.5406	1.1784	1.1552

Table 6. Error in the prediction of chopping ratio from ANN controller for MP operation

% Of solar insolation	% Error in the prediction for volumetric pump load	% Error in the prediction for centrifugal pump load
10	−6.67	−1.15
15	−5.83	−0.17
20	−1.03	2.08
25	−2.24	−1.45
30	−0.19	−0.51
35	1.03	0.56
40	−0.41	−0.87
45	2.12	−0.15
50	0.86	0.49
55	1.22	1.14
60	−0.01	0.09
65	0.29	0.30
70	0.54	0.35
75	−0.41	−0.68
80	−0.14	−0.43
85	0.09	0.26
90	−0.62	−0.94
95	−0.31	−0.17
100	−0.02	1.25

Table 7. Error in the prediction of chopping ratio from ANN controller for GME operation

% Of solar insolation	% Error in the prediction for volumetric pump load	% Error in the prediction for centrifugal pump load
10	−5.28	−0.27
15	−5.26	−0.18
20	−0.87	1.56
25	−2.31	−1.65
30	−0.42	−0.16
35	0.75	1.25
40	−0.78	−0.37
45	−0.04	−0.34
50	0.46	−0.34
55	0.83	0.25
60	−0.36	−0.24
65	−0.01	0.72
70	0.29	1.02
75	−0.62	−0.51
80	−0.28	−1.00
85	0.04	−0.88
90	−0.61	−1.11
95	−0.21	0.19
100	0.18	1.97

NOMENCLATURE

A	Completion factor
A_1	Torque constant of rotational losses
B_1	Viscous torque constant
C_e	Flux coefficient
E_b	Back emf at MP operation
E^*_b	Back emf at GME operation
I_g	SCA current
I_m	SCA current at MP operation
I_{av}	Average motor armature current for MP operation
I^*_{av}	Average motor current for GME operation
I_{ph}	Insolation dependent photo current
I_{og}	Cell reverse saturation current
J	Moment of inertia
K	Boltzman constant
K_{ins}	Percentage of Solar insolation
L_a	Armature circuit inductance
N_p	No. of parallel cells in SCA
N_s	No. of series cells in SCA
P_g	SCA power output
P_m	SCA power at MP operation
P^*_m	SCA power at GME operation
R_a	Armature circuit resistance
T	Absolute temperature
T_l	Load torque
T_e	Electromagnetic Torque developed
t_{on}	On-time of the switch
T_p	Switching period of the converter
V_g	SCA Voltage
V_m	SCA Voltage at MP operation
V^*_m	SCA Voltage at GME operation
V_{av}	Average motor armature voltage for MP operation
W^h_{ji}	Weight on the connection from i^{th} input unit
Y	Chopping ratio
Y_{MP}	Chopping ratio for MP operation
Y_{GME}	Chopping ratio for GME operation
ω	Angular speed
δ	Duty ratio
δ_{mp}	Duty ratio for MP operation
δ^*_{mg}	Duty ratio for GME operation
θ^h_j	Bias for hidden layer neurons

Acknowledgements—The authors are thankful to Jawaharlal Nehru Technological University authorities for supporting this research and also thankful to the reviewers for their valuable remarks and suggestions.

REFERENCES

Appelbaum J. (1986) Starting and steady-state characteristics of dc motors powered by solar cell generators. *IEEE Trans. on Energy Conversion* **1**, 17–24.

Haykin S. (1994). *Neural Networks-A comprehensive Foundation*, Macmillan, New York.

Freeman J. A. and Skapura D. M. (1991). *Neural Networks, algorithms, applications and programming techniques*, Wesley Publishing Inc, Addision.

Narendra K. S. and Parthasarathy K. (1990) Identification and control of dynamical systems using neural networks. *IEEE Trans. on Neural Networks* **1**(1), 4–27.

Saied M. M. (1988) Matching of dc motors to photovoltaic generators for maximum daily gross mechanical energy. *IEEE Trans. on Energy Conversion* **3**, 465–472.

PDP group Eds, Rumelhart D. E., Hinton G. E. and Williams R. J. (1986). In *Learning internal representations by error propagation, parallel distributed processing*, pp. 318–362.

Takashi H. and Imakubo T. (1995) Identification of optimal operating point of PV modules using neural network for real time maximum power tracking control. *IEEE Trans. on Energy Conversion* **10**(2), 360–367.

Veerachary M. (2000) Steady state and dynamic performance of PV supplied dc motors fed from intermediate power converters. *Solar Energy Materials and Solar Cells* **61**, 365–381.

Widrow B. and Lehr M. A. (1990) 30 years of adaptive neural networks: Perceptron, Madaline and back propagation. *Proceedings of IEEE* **78**(9), 1415–1442.

Zinger Z. and Braunstein A. (1981) Optimum operation of a combined system of a solar cell array and a dc motor. *IEEE Trans. on PAS* **100**, 1193–1197.